M R S Internet Journal of Nitride Semiconductor Research

Volume 1, Article 8

Growth, Doping and Characterization of $Al_xGa_{1-x}N$ Thin Film Alloys on 6H-SiC(0001) Substrates

M. D. Bremser, W. G. Perry, T. Zheleva, N. V. Edwards, O. H. Nam
Department of Materials Science and Engineering, North Carolina State University

N. Parikh
University of North Carolina at Chapel Hill Department of Physics and Astronomy

D. E. Aspnes
Department of Physics, North Carolina State University

Robert F. Davis
Department of Materials Science and Engineering, North Carolina State University

This article was received on July 23, 1996 and accepted on September 10, 1996.

Abstract

Thin films of $Al_xGa_{1-x}N$ ($0.05 \leq x \leq 0.96$) having smooth surfaces were deposited directly on both vicinal and on-axis 6H-SiC(0001) substrates. Cross-sectional TEM of $Al_{0.13}Ga_{0.87}N$ revealed stacking faults near the SiC/Nitride alloy interface and numerous threading dislocations. EDX, AES and RBS were used to determine the compositions, which were paired with their respective CL near band-edge emission energies. A negative bowing parameter was determined. The CL emission energies were similar to the bandgap energies obtained by SE. FE-AES of the initial growth of $Al_{0.2}Ga_{0.8}N$ revealed an aluminum rich layer near the interface. N-type (silicon) doping was achieved for $Al_xGa_{1-x}N$ for $0.12 \leq x \leq 0.42$. $Al_{0.2}Ga_{0.8}N$/GaN superlattices were fabricated with coherent interfaces. Additionally, HEMT structures using an AlN/GaN/AlN buffer structure were fabricated.

1. Introduction

The potential and employment of III-Nitride materials for both optoelectronic and microelectronic applications has stimulated significant research. [1] The wurtzitic phase of GaN forms continuous solid solutions with InN and AlN such that bandgap engineering is possible from 1.95 eV to 6.2 eV. When alloyed solely with AlN, materials having bandgaps from 3.4 eV to 6.2 eV are possible. This makes $Al_xGa_{1-x}N$ attractive for both ultraviolet emitters and detectors as well as high-power and high-frequency microelectronic applications.

Single crystal GaN substrates are currently available in very limited quantities only via high pressure, high temperature processes. [2] As such, heteroepitaxy is the dominant growth process, and c-plane sapphire is the most commonly employed substrate. In order to accommodate the large lattice mismatch between GaN and sapphire, nitridation of the latter followed by the deposition of a low temperature amorphous GaN or AlN buffer layer is conducted prior to GaN film growth. [3] [4] This buffer layer is subsequently annealed to form a textured polycrystalline template upon which the GaN is deposited. Grain orientation competition in the GaN film occurs during the first 0.5 microns of growth which results in the formation of low angle grain boundaries which persist throughout the entire epitaxial layer. [5] Substantial concentrations of threading dislocations exist near the film/buffer layer interface, some of which are annihilated by intersection within the film. As such, the growth of 3 to 4 microns of material is usually necessary to achieve "device quality" epitaxy. In contrast, it has been shown that monocrystalline AlN can be deposited epitaxially on 6H-SiC(0001) at temperatures >1050°C [6] [7] Use of a 1000Å AlN buffer layer deposited at 1100°C has been demonstrated to be an effective buffer layer [6] [7] Subsequent

GaN epitaxy also contains random threading dislocations but is free of low angle grain boundaries. Despite the close lattice match of 6H-SiC(0001) and GaN (3.5%), the use of a buffer layer is necessary for organometallic vapor phase epitaxy (OMVPE) since the two-dimenional growth of thick (>1 micron), smooth GaN directly on 6H-SiC has not been demonstrated. Since highly conductive AlN has yet to be demonstrated, the AlN buffer layer prohibits the effective use of the conductive SiC for the formation of backside contacts. Hence, the use of a conductive $Al_xGa_{1-x}N$ as a buffer layer appears to hold more promise. In this research, the deposition, doping and characterization of $Al_xGa_{1-x}N$ thin films growth directly on 6H-SiC(0001) wafers has been extensively studied and will be reported in the following sections.

2. Experimental Procedures

Thin films of $Al_xGa_{1-x}N$ were deposited at 1050-1150°C and 45 Torr in a cold-wall, vertical, pancake-style, RF inductively heated, OMVPE system using various ratios of triethylaluminum (TEA) and triethylgallium (TEG) in combination with 1.5 SLM of ammonia (NH_3) and 3 SLM of H_2 diluent. The total metalorganic precursor flow rate was 32.8 micromoles/min. Donor and acceptor type doping was accomplished by the addition of SiH_4 and Cp_2Mg, respectively. Additional experimental parameters are described elsewhere [6] [7]

The structural, microstructural, optical and electrical characteristics of the epitaxial $Al_xGa_{1-x}N$ thin films were analyzed using several techniques. Scanning electron microscopy (SEM) was performed using a JEOL 6400FE operating at 5 kV and equipped with an Oxford Light Element Energy Dispersive X-ray (EDX) Microanalyzer. Conventional and high resolution transmission electron microscopies (TEM) were conducted using a Topcon EM- 002B microscope operating at 200 kV. Double-crystal x-ray rocking curve (DCXRC) measurements were made on a Philips MR3 thin films diffractometer. Atomic Force Microscopy (AFM) was performed on a Digital Instruments Dimension 3000. The catholuminescence (CL) properties of the $Al_xGa_{1-x}N$ films were determined at 4.2 K using a Kimball Physics EMG-14 electron gun as the excitation source. Spectroscopic ellipsometry (SE) was performed using a rotating analyzer ellipsometer with a xenon arc lamp (1.5eV - 5.75eV). Capacitance- Voltage (CV) measurements were conducted using a MDC Model CSM/2-VF6 equipped with a mercury probe. Standard and field emission Auger electron spectropies (AES and FE-AES) were conducted using Perkin-Elmer Models 660 and 670, respectively, equipped with Zalar rotation. Rutherford backscattering analysis (RBS) was performed using 1.9 MeV He^+ ions with the detector at an angle of 165°.

3. Results and Discussion

Thin films of $Al_xGa_{1-x}N$ ($0.05 \leq x \leq 0.96$) were deposited directly on both vicinal and on-axis 6H-SiC(0001) substrates. As shown in Figures 1 and 2, films having $x < 0.5$ and deposited at 1100°C had smooth, featureless surfaces. SEM also revealed that, like GaN, smoother films were deposited on the on-axis substrates than on the vicinal ones. The surfaces of films with $x > 0.5$ were also very smooth but with occasional pits which increased in density with increasing Al composition. The occurrence of pits likely indicates the lack of surface mobility of the metal adatoms such that complete crystallographic coalescence of the two dimensional flat-top islands is inhibited. [6] [7] In order to eliminate this problem, deposition of the $Al_xGa_{1-x}N$ for $x > 0.5$ was conducted at 1150°C. The resulting films possessed smooth surfaces which were free of pits; however, the growth rate decreased by more than a factor of three. Therefore, deposition in the range of 1120-1130°C is likely optimum for our system for these higher AlN concentrations.

The compositions of the films grown under different conditions were determined using EDX**,** AES and RBS. Standards of AlN and GaN grown in the same reactor under similar conditions were used for the EDX and AES analyses. Compositions were assigned to each film after carefully consideration of the errors (2 at.%) involved with each technique. The data from EDX and AES measurements showed excellent agreement. AES (detection limit ≈ 1 at.%) did not reveal any oxygen or carbon in the bulk of these films. The RBS data did not agree as well with the other two techniques due to small compositional variations through the thickness of the film. Simulation of the compositions determined by RBS was conducted only for the surface compositions. Analysis via EDX revealed that the $Al_xGa_{1-x}N$ grown on the on-axis SiC substrates tended to be 1-2 atomic percent more Al rich than those grown off-axis SiC. It is thought that the presence of steps on the growth surface promotes the adhesion of the gallium adatoms. Composition determination using x-ray diffraction and Vegard's Law was not employed due to the strained state of these films which will be discussed in the following sections.

In Figure 3, these compositions are compared with their respective CL near band-edge emission energies. Additionally, in Figure 4, the CL emission peaks are compared with bandgap values obtained by SE. Using a parabolic model, the following relationships describe the CL peak emission (I_{PL} line emission) (Eq (1)) as a function

parabolic model, the following relationships describe the CL peak emission (I_2-line emission) (Eq.(1)) as a function aluminum mole fraction for 0 < x < 0.96.

$$E_{I2}(x) = 3.50 + 0.64x + 1.78x^2 \quad (1)$$

Clearly, the model of the measurements shows a negative deviation from a linear fit. This is in agreement with earlier research by other investigators. [8] [9] [10] However, these films are highly strained due to incomplete relaxation of the tensile stresses generated by the differences in the coefficients of thermal expansion. The effect of strain has yet to be quantified. It should be noted that other researchers have seen a linear relationship between composition and absorption edge for thick or relaxed films on sapphire. [11] [12] Comparison of the CL spectra of $Al_{0.12}Ga_{0.88}N$ grown on a pre-deposited 1000Å AlN buffer layer which is used for GaN deposition versus growth directly on 6H-SiC reveals a 75 meV red shift for the latter films (Figure 5). This indicates that the films deposited directly on SiC are in greater tension than the ones deposited using an AlN buffer layer. Furthermore, there is a noticeable decrease in the defect peak centered around 3.2 eV. The reason for the reduction in this peak is unclear at this time and is under investigation.

The low temperature (4.2K) CL of undoped $Al_xGa_{1-x}N$ films containing up to 0.96 mole fraction of aluminum exhibited near band-edge emission which has been attributed to an exciton bound to a neutral donor (I_2-line emission). [13] For increasing concentrations of aluminum, this emission became gradually weaker. No emission was observed for pure AlN other than a broad peak centered around 3.1 eV which has been previously attributed to oxygen. [14] The most narrow near band-edge CL FWHM was 31 meV for $Al_{0.05}Ga_{0.95}N$. This value increased with aluminum concentration to a maximum of approximately 100meV for $Al_{0.5}Ga_{0.5}N$. For higher aluminum compositions, this value did not increase. The broadening of the exciton features is likely due to both exciton scattering in the alloy as well as small variations in alloy compositions in the film. Additionally, two strong defect peaks were present at energies less than the band gap. Both of these features have been previously attributed to donor-acceptor transitions. The first peak is centered around 2.2 eV for GaN and is commonly associated with deep levels in the bandgap. [15] As shown in Figure 6, these emissions changed sublinearly with changing composition. The nature of this behavior is under investigation. The second defect peak is centered around 3.27 eV which is attributed to a transistion between a shallow donor and a shallow acceptor, [16] and its position also changes sublinearly with increasing aluminum concentration, as shown in Figure 7. This sublinear shift is attributed to the donor state moving deeper into the gap. For $Al_{0.05}Ga_{0.95}N$, the donor to acceptor pair (DAP) and its two LO-phonon replicas typically seen in GaN are still resolved, but for higher aluminum compositions, these peaks become one broad peak. Furthermore, for films deposited at 1150°C, this peak is no longer seen in the CL spectra. Increasing the growth temperature to eliminate this defect peak would indicate that it is impurity related. Attempts to determine this impurity are in progress.

Initial studies of the initial growth of $Al_xGa_{1-x}N$ directly on SiC give some insight into the strain relief mechanisms near the $Al_xGa_{1-x}N$/SiC interface. Despite the somewhat close lattice match between GaN and 6H-SiC(0001) (3.5%), previous research in our laboratories has shown that GaN epitaxy undergoes three dimensional island growth, since the critical thickness of GaN on 6H-SiC is <10Å. By contrast, AlN films, with a critical thickness of 45Å and a lattice mismatch of 0.9%, grow via coalescence of two dimensional flat-top islands which gradually roughens with increasing thickness. [17] At a thickness of 1000Å, AFM measurements reveal an RMS roughness of 32Å (Figure 8) when deposited on vicinal SiC substrates.

In contrast, $Al_xGa_{1-x}N$ films deposited at 1050°C undergo a considerably more complex growth mechanism. Figure 9 shows the results of five minutes of deposition with a gas phase mixture which results in a $Al_{0.2}Ga_{0.8}N$ thin film. It clearly shows two distinct regions of growth which are referred to as the "islands" and the "valleys". The compositions of the islands and the valleys were determined using FE-AES(Figure 10). Two important findings are evident from this graph. Firstly, this data clearly shows that the interface region is aluminum rich and that the bulk film composition is achieved at approximately 100Å of film thickness. Secondly, the interface of the valley regions is significantly more aluminum rich than the islands. The valley regions appear to contain approximately 0.65 mole fraction of aluminum at the interface while the islands contains only 0.40 mole fraction of aluminum at the interface. Assuming Vegard's Law, this would imply an interfacial mismatch of only 1.9% for the valleys versus 2.5% for the islands. It should be noted that the mismatch of the islands is the same as that between AlN and GaN and, moreover, their morphology is similar to that observed for the first few hundred angstroms of GaN deposited on a high temperature AlN buffer layer. [7] The process of coalescence results in smooth $Al_xGa_{1-x}N$ films similar to that shown in Figures 1 and 2 after a few thousands angstroms of growth. It should be noted that profiling took place in 100Å increments. Therefore, the possibility exists that an extremely thin AlN or aluminum rich $Al_xGa_{1-x}N$ layer occurs within the first few angstroms of the interface; thereby providing a graded buffer layer structure of less than 100Å in thickness. More noteable, however, is the fact that low temperature CL revealed near band-edge emission at 3.53

eV. This indicates that a tremendous amount of tensile strain is present in this film since thicker films of the same composition have emission located at 3.83 eV. In summary, initial studies indicate that lattice strain is partial relieved at the interface during growth by the formation of an aluminum rich buffer layers which result in an island morphology. Subsequently, these islands coalescence into a smooth, coherent film containing tensile strain generated during cooling due to the differences in the thermal expansion coefficents as well as numerous threading dislocations.

The TEM micrograph in Figure 11 of a 1.8 micron thick $Al_{0.13}Ga_{0.87}N$ film deposited on an on-axis substrate revealed a microstructure dominated by threading dislocations, but free of low angle grain boundaries. Inspection of this and other micrographs reveals a progressive reduction in dislocation density as one moves away from the $Al_xGa_{1-x}N$/SiC interface. This is additionally supported by a narrowing of the full width at half maximum (FWHM) of the DCXRC of the $Al_{0.13}Ga_{0.87}N$ (0002) peak from 315 arcsec to 186 arcsec as the thickness of film increased from 0.9 microns to 1.8 microns. For films of similar thicknesses and compositions, films grown on vicinal SiC substrates exhibited higher FWHMs of the DCXRC of the AlGaN(0002). Furthermore, the growth rate on vicinal substrates was slightly higher due to increased density of steps on the surface; however, these steps probably act as formation sites for inversion domain boundaries. [17] Additionally, TEM revealed, as shown in Figure 12, the presence of planar defects located parallel to the interface in the first few hundred angstroms of the $Al_xGa_{1-x}N$ films.

Several structures have been grown using GaN and $Al_xGa_{1-x}N$. A TEM micrograph of an $Al_{0.2}Ga_{0.8}N$/GaN superlattice with periods of various thicknesses is shown in Figure 13. A schematic of the structure is shown in Figure 13a. The superlattice structure was deposited on 0.6 microns GaN which was deposited on a 1000Å, 1100°C AlN buffer layer. Each superlattice period was repeated 5 times and the structure was capped with 0.2 microns of GaN. Figures 13b and 13c shows coherent interfaces and the high quality of the superlattice structure. Observation of the structure in plan-view TEM did not indicate a reduction in dislocation density below that normally observed in single layer GaN films on a buffer layer. In Figure 14, a TEM cross-section of a high electron mobility transistor (HEMT) device is shown. Growth was initiated similarly to the previous structure, but a second, 500Å AlN layer was used both to allow pinch-off of the device as well as to improve the quality of the GaN active layer. Results of device operation will be reported at a later date.

Undoped, high quality $Al_{0.05}Ga_{0.95}N$ films grown directly on vicinal 6H- SiC(0001) exhibited residual, ionized donor concentrations of 1×10^{18} cm^{-3}. The ionized donor concentration decreased rapidly with increasing Al content and was $<1 \times 10^{17}$ cm^{-3} for $Al_{0.12}Ga_{0.88}N$ and $<1 \times 10^{16}$ cm^{-3} for $Al_{0.35}Ga_{0.65}N$, as determined by CV measurements. The origin of these donors is under investigation, since concentrations of $<1 \times 10^{15}$ cm^{-3} have been measured for GaN films grown on AlN buffer layers in the same reactor. Moreover, layers of undoped AlN having N_D-N_A of 8×10^{15} cm^{-3} has also been deposited. However, the controlled introduction of SiH_4 allowed the reproducible achievement of ionized donor concentrations within the range of 2×10^{17} cm^{-3} to 2×10^{19} cm^{-3} in $Al_xGa_{1-x}N$ films for $0.12 \leq x \leq 0.42$. For $x > 0.42$, additions of silicon resulted in films too resistive for CV measurements. The growth of p-type $Al_xGa_{1-x}N$ films for $x \leq 0.13$ via the introduction of Mg has been successful.

4. Conclusions

Thin films of $Al_xGa_{1-x}N$ ($0.05 \leq x \leq 0.96$) having smooth surfaces were deposited directly on vicinal and on-axis 6H-SiC(0001) substrates. Cross-sectional TEM of $Al_{0.13}Ga_{0.87}N$ revealed a microstructure similar to that of GaN grown on a high-temperature AlN buffer layer. EDX, AES and RBS were used to determine the compositions.which were paired with their respective CL near bandedge emission energies. A negative bowing parameter was determined. The CL emission energies were similar to the bandgap values obtained by SE. FE-AES of the initial growth of $Al_{0.2}Ga_{0.8}N$ revealed an aluminum rich layer near the interface. $Al_{0.2}Ga_{0.8}N$/GaN superlattices with coherent interfaces were fabricated. Additionally, HEMT structures using AlN/GaN/AlN buffer structures were demonstrated. N-type (silicon) doping was achieved for $Al_xGa_{1-x}N$ for $0.12 \leq x \leq 0.42$.

Acknowledgments

The authors express their appreciation to Cree Research, Inc. of Durham, North Carolina for providing the SiC wafers and Mr. T. Warren Weeks, Jr., Dr. A.D. Batchelor and Dr. K. Hiramsutsu for their contributions and fruitful discussions. This research was supported by the Office of Naval Research

under Contract N00014-092-J-1477.

References

[1] S. Strite, H. Morkoç, *J. Vac. Sci. Technol. B* ***10***, 1237-1266 (1992).

[2] M. Leszczynski, H. Teisseyre, T. Suski, I. Grzegory, M. Bockowski, J. Jun, S. Porowski, K. Pakula, J. M. Baranowski , C. T. Foxon, T. S. Cheng , *Appl. Phys. Lett.* ***69***, 73-75 (1996).

[3] S. Nakamura, M. Senoh, T. Mukai, *Jpn. J. Appl. Phys.* ***30***, L1708 (1991).

[4] H. Amano, I. Akasaki, K. Hiramatsu, N. Koide, N. Sawaki, *Thin Sol. Films* ***163***, 415 (1988).

[5] W. Qian, M. Skowronski, M. De Graef , K. Doverspike, L. B. Rowland, D. K. Gaskill , *Appl. Phys. Lett.* ***66***, 1252-1254 (1995).

[6] T. Warren Weeks, Michael D. Bremser, K. Shawn Ailey, Eric Carlson, William G. Perry, Robert F. Davis, *Appl. Phys. Lett.* ***67***, 401-403 (1995).

[7] T.W. Weeks, M.D. Bremser, K.S. Ailey, E.P. Carlson, W.G. Perry, E.L. Piner, N.A. El-Masry, R.F. Davis, *J. Mater. Res.* ***11***, 1081 (1996).

[8] S. Yoshida, S. Misawa, S. Gonda, *J. Appl. Phys.* ***53***, 6844 (1982).

[9] Y. Koide, H. Itoh, M. R. H. Khan, K. Hiramatu, N. Sawaki, I. Akasaki , *J. Appl. Phys.* ***61***, 4540-4543 (1987).

[10] M.R.H. Khan, Y. Koide, H. Itoh, N. Sawaki, I. Akasaki, *Sol. St. Comm.* ***60***, 509 (1986).

[11] D. K. Wickenden, C. B. Bargeron, W. A. Bryden, J. Miragliotta, T. J. Kistenmacher, *Appl. Phys. Lett.* ***65***, 2024-2026 (1994).

[12] M. A. Khan, R. A. Skogman, R. G. Schulze, M. Gershenzon, *Appl. Phys. Lett.* ***43***, 492 (1983).

[13] R. Dingle, D. D. Sell, S. E. Stokowski, M. Ilegems, *Phys. Rev. B* ***4***, 1211 (1971).

[14] I. Adams, T.R. AuCoin, G.A. Wolff, *J. Electrochem.Soc.* ***109***, 1050 (1962).

[15] W. Gotz, N. M. Johnson, R. A. Street , H. Amano, I. Akasaki , *Appl. Phys. Lett.* ***66***, 1340-1342 (1995).

[16] R. Dingle, M. Ilegems, *Sol. St. Comm.* ***9***, 175 (1971).

[17] S Tanaka, RS Kern, RF Davis, *Appl. Phys. Lett.* ***66***, 37 (1995).

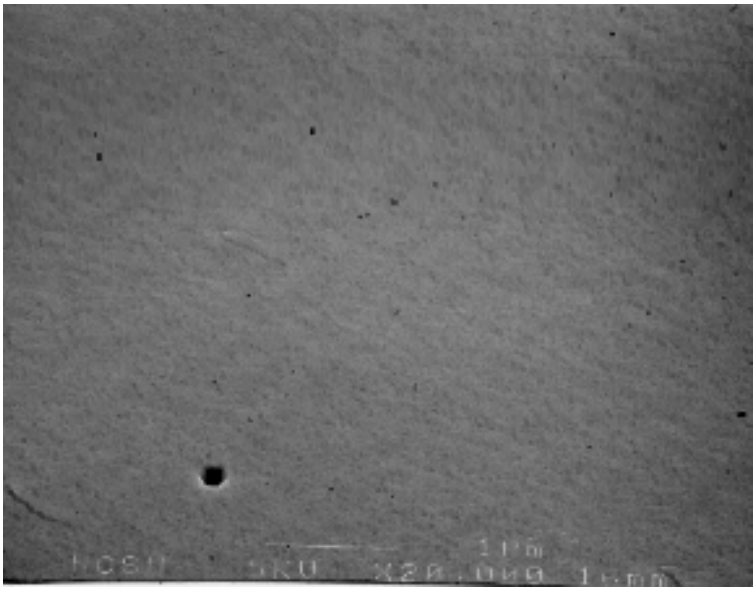

Figure 1. SEM micrograph of a 0.5 μm $Al_{0.41}Ga_{0.59}N$ film deposited directly on a vicinal 6H-SiC (0001) substrate.

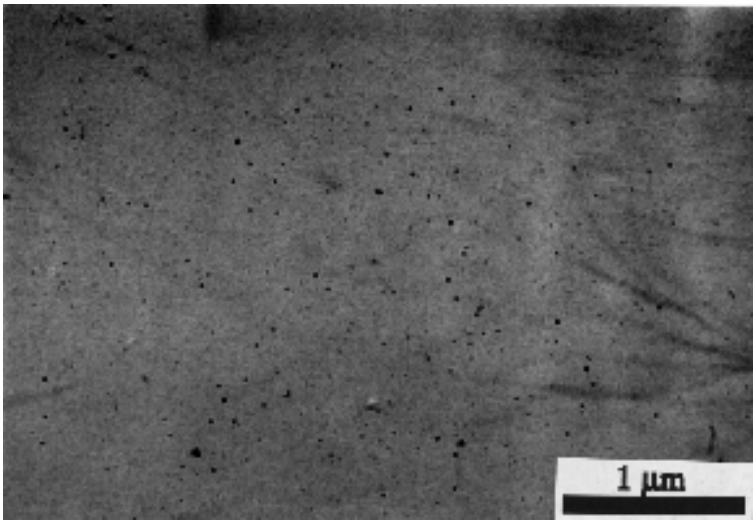

Figure 2. SEM micrograph of a 0.8 μm $Al_{0.13}Ga_{0.87}N$ film deposited directly on an on-axis 6H-SiC (0001) substrate.

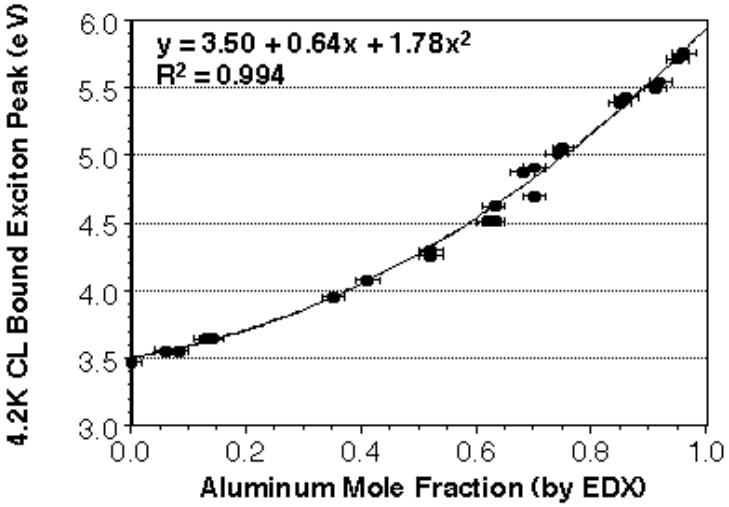

Figure 3. The relationship between aluminum mole faction and 4.2K CL near band-edge emission from AlGaN thin films deposited directly on vicinal and on-axis 6H-SiC (0001) substrates.

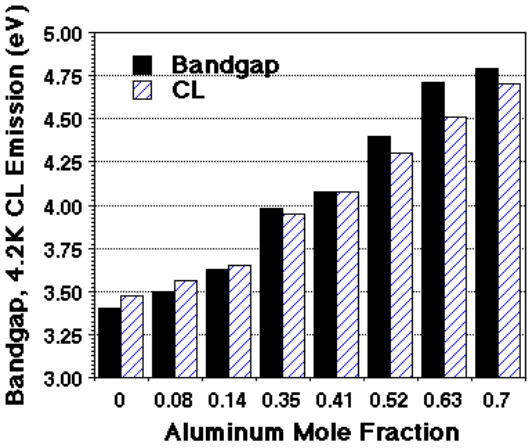

Figure 4. Comparsion of 4.2K CL near band-edge emission and bandgap as determined by spectroscopic ellipsometry at room temperature.

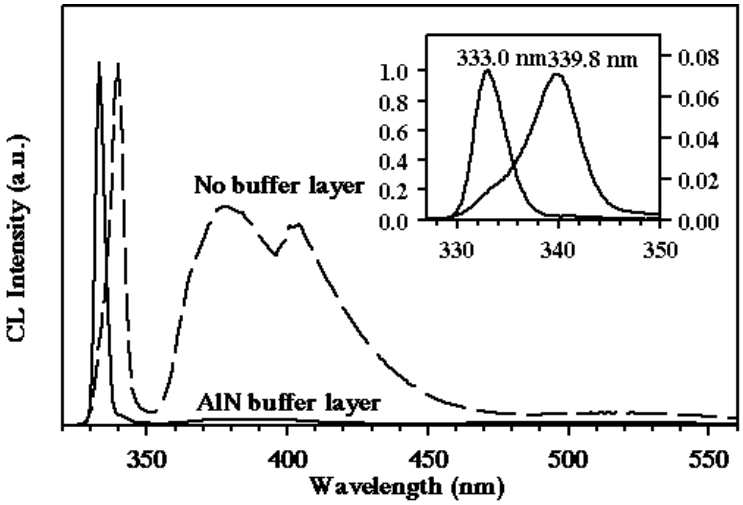

Figure 5. Comparsion of 4.2K CL spectra of $Al_{0.12}Ga_{0.88}N$ deposited directly on 6H-SiC and using a 1000Å AlN buffer layer.

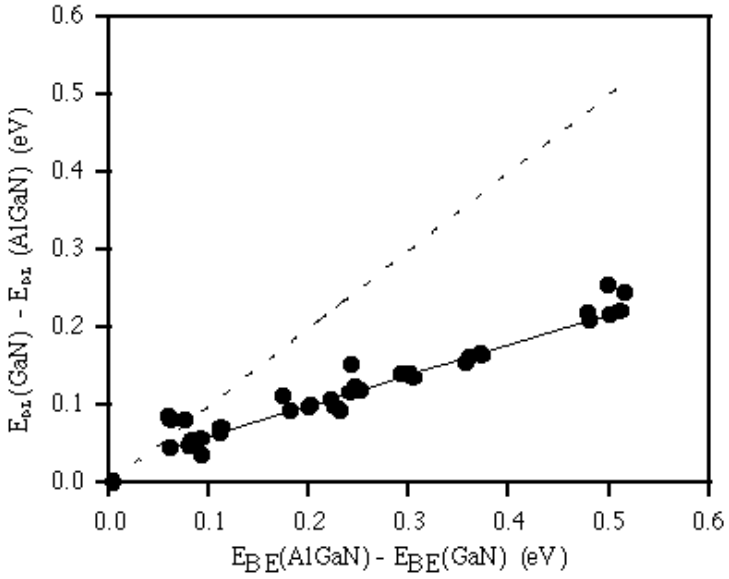

Figure 6. The sublinear shift in the deep level emission (“yellow luminescence») as a function of the increase in 4.2K CL near band-edge emission.

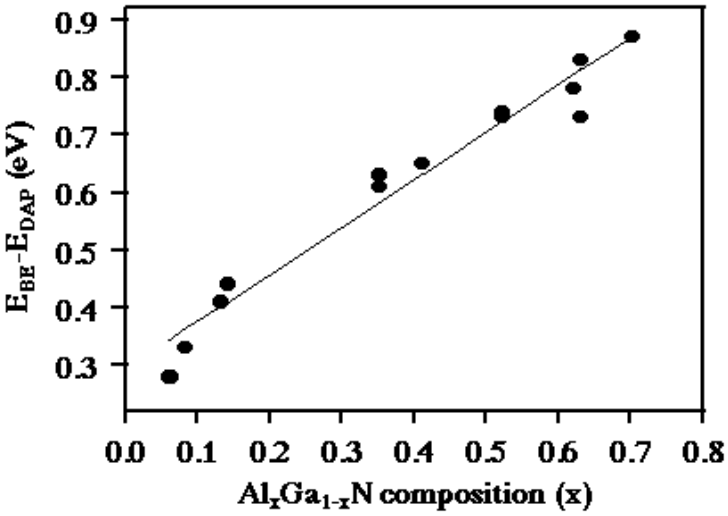

Figure 7. The difference in 4.2K CL near band-edge emission and the shallow donor to shallow acceptor (DAP) peak position as a function of aluminum mole fraction.

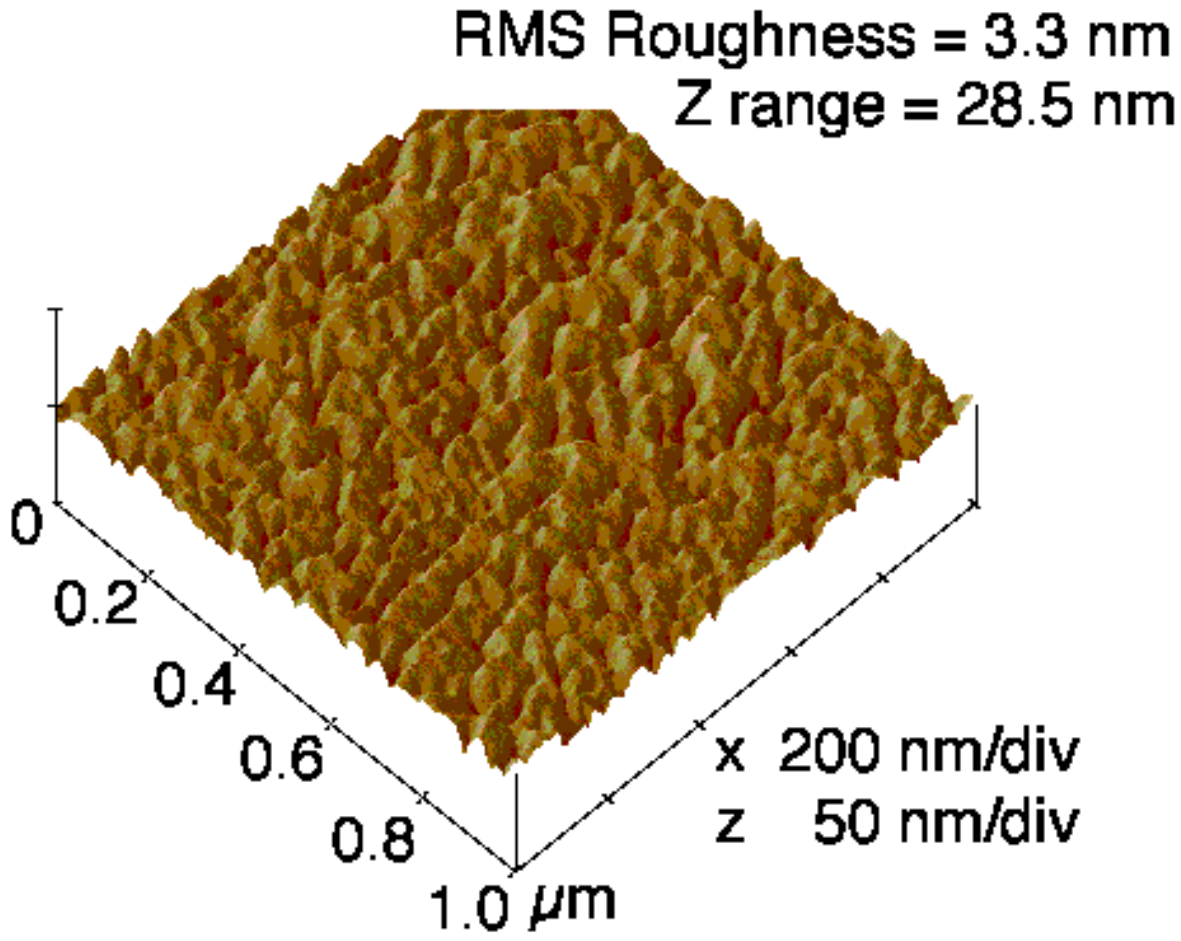

Figure 8. AFM of a 1000Å AlN buffer layer deposited on vicinal 6H-SiC.

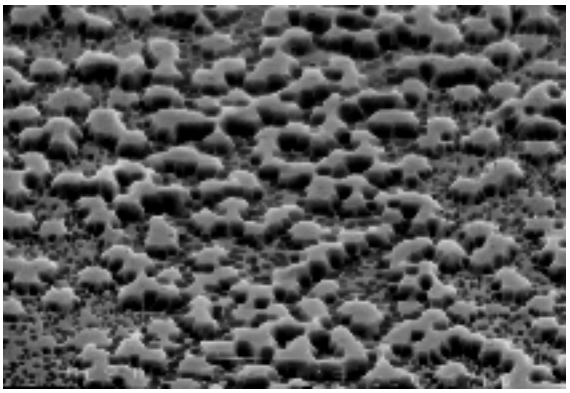

Figure 9. SEM of 5 minutes of growth of $Al_{0.2}Ga_{0.8}N$ at 1050C directly on 6H-SiC.

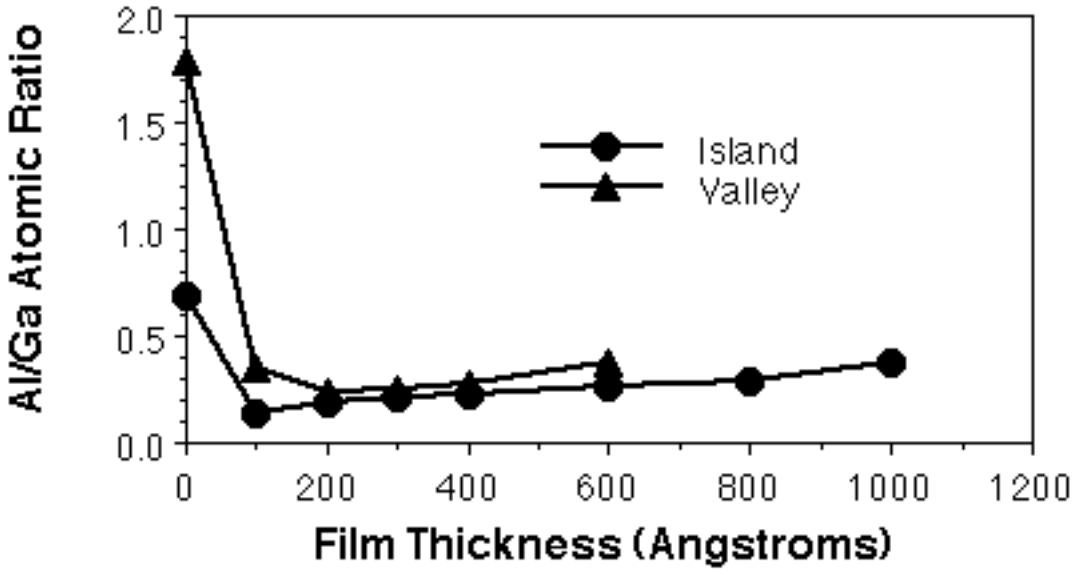

Figure 10. FE-AES of the various areas of the sample shown in Figure 9.

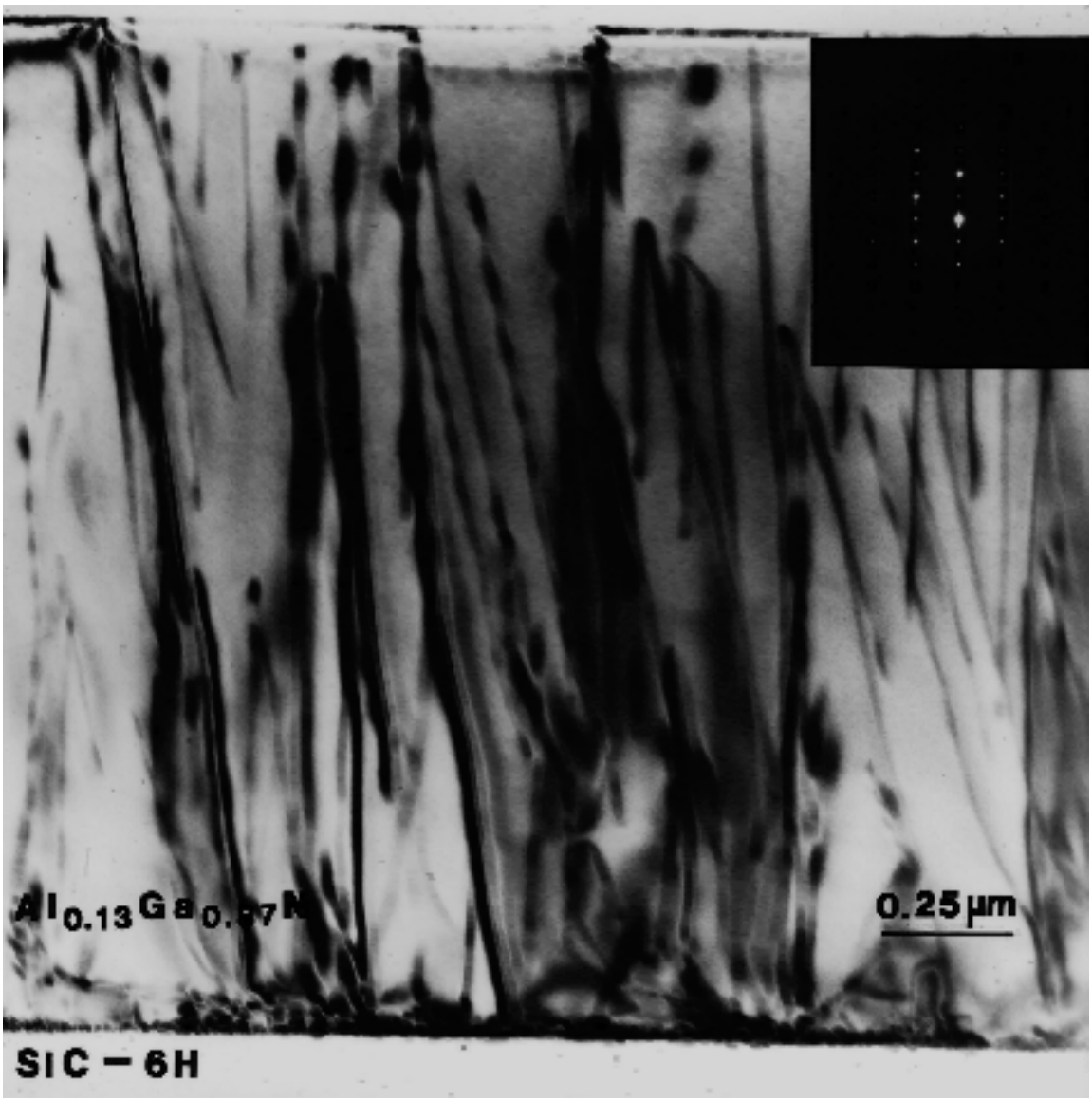

Figure 11. Cross-sectional TEM micrograph of 1.8µm AlGaN (0001) film deposited at 1100C and 45 Torr directly on 6H-SiC (0001) substrate. The inset shows the selected area diffraction.

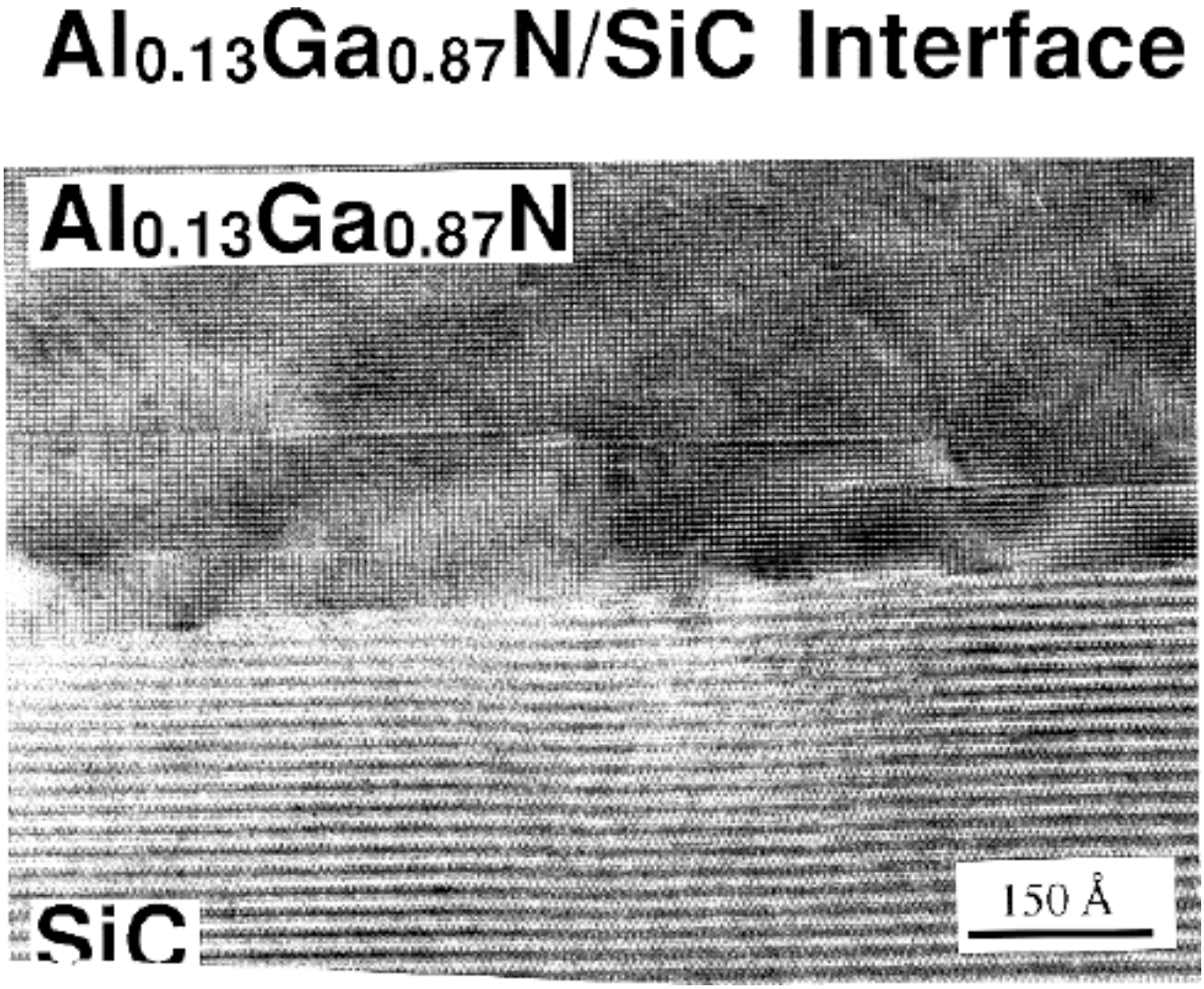

Figure 12. Cross-sectional TEM micrograph of interface region of 1.8μm AlGaN (0001) film deposited at 1100C and 45 Torr directly on 6H-SiC (0001) substrate.

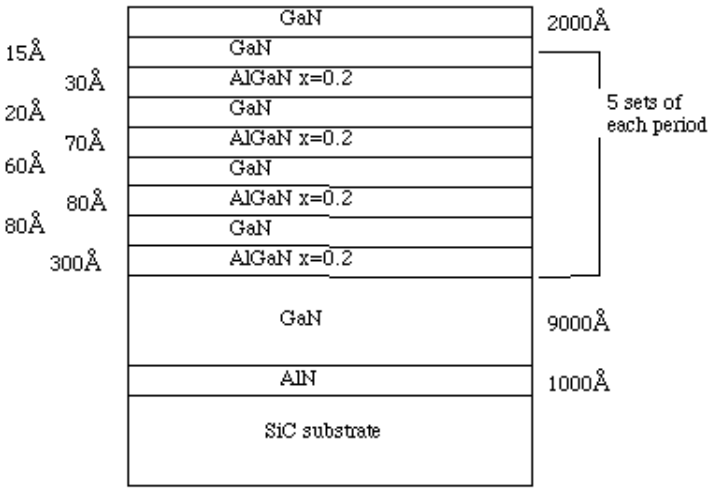

Figure 13. a) A schematic of a superlattice structure grown on 6H-SiC. b) A cross-section TEM micrograph showing the superlattice region of the structure. c) A high resolution, cross-sectional TEM micrograph showing the 15Å GaN/30Å AlGaN periods.

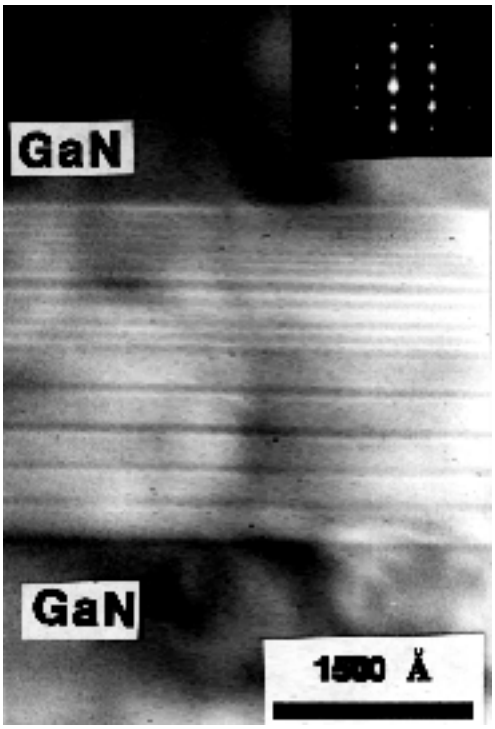

Figure 13a. a) A schematic of a superlattice structure grown on 6H-SiC. b) A cross-section TEM micrograph showing the superlattice region of the structure. c) A high resolution, cross-sectional TEM micrograph showing the 15Å GaN/30Å AlGaN periods.

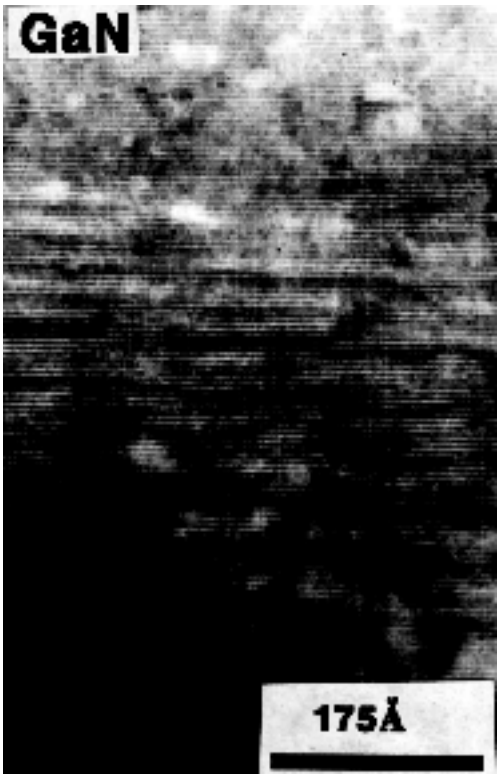

Figure 13b. a) A schematic of a superlattice structure grown on 6H-SiC. b) A cross-section TEM micrograph showing the superlattice region of the structure. c) A high resolution, cross-sectional TEM micrograph showing the 15Å GaN/30Å AlGaN periods.

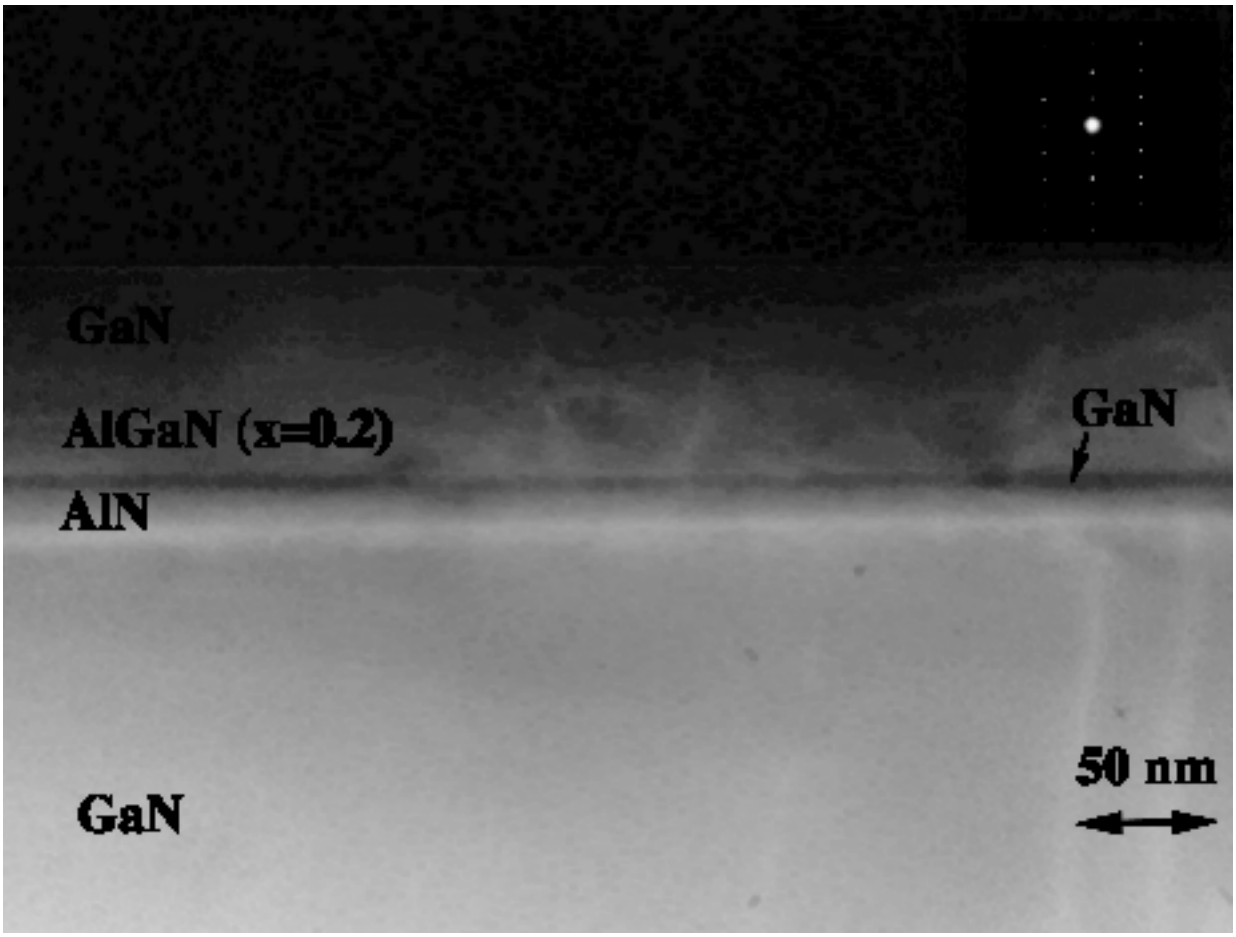

Figure 14. A cross-sectional TEM micrograph of a HEMT device.

M R S Internet Journal of Nitride Semiconductor Research